

# Anisotropic upper mantle structures in northeast Asia from Bayesian inversions of ambient noise data

EGU2020-6466

© Authors. All rights reserved

<sup>1</sup>School of Earth and Environmental Sciences, Seoul National University, Seoul, Korea. <sup>2</sup>Department of Geology & Earth Environmental Sciences, Chungnam National University, Daejeon, Korea



## Abstract

The northeast Asia region exhibits complex tectonic settings caused by interactions between Eurasian, Pacific, and Philippine Sea plates. Distributed extensional basins, intraplate volcanoes and other heterogeneous features in the region marked results of the tectonic processes, and their mechanisms related to mantle dynamics can be well understood by estimating radial anisotropy in the lithospheric and asthenospheric. We constructed a three-dimensional radial anisotropy model in northeast Asia using hierarchical and transdimensional Bayesian joint inversion techniques with different types of dispersion data up to the depth of the upper mantle (~160 km). Thick and deep layers with positive radial anisotropy ( $V_{SH} > V_{SV}$ ) were commonly found at depths between 70 and 150 km beneath the continental regions. On the other hand, depths and sizes of layers with positive radial anisotropy become shallower and thinner (30 ~ 60 km) respectively beneath regions where experienced the Cenozoic extension. These variations in positive radial anisotropy for different tectonic regions can be understood with the context of extensional geodynamic processes in back arc basins within the East Sea (Japan Sea). Interestingly, the most predominant positive radial anisotropy is imaged along areas with large gradient of the lithosphere-asthenosphere boundary beneath intraplate volcanoes. These observations favor the mechanism of edge-driven convection caused by the difference in lithosphere thickness and localized sublithospheric lateral flow from the continental region to back arc basins.

## Data and process

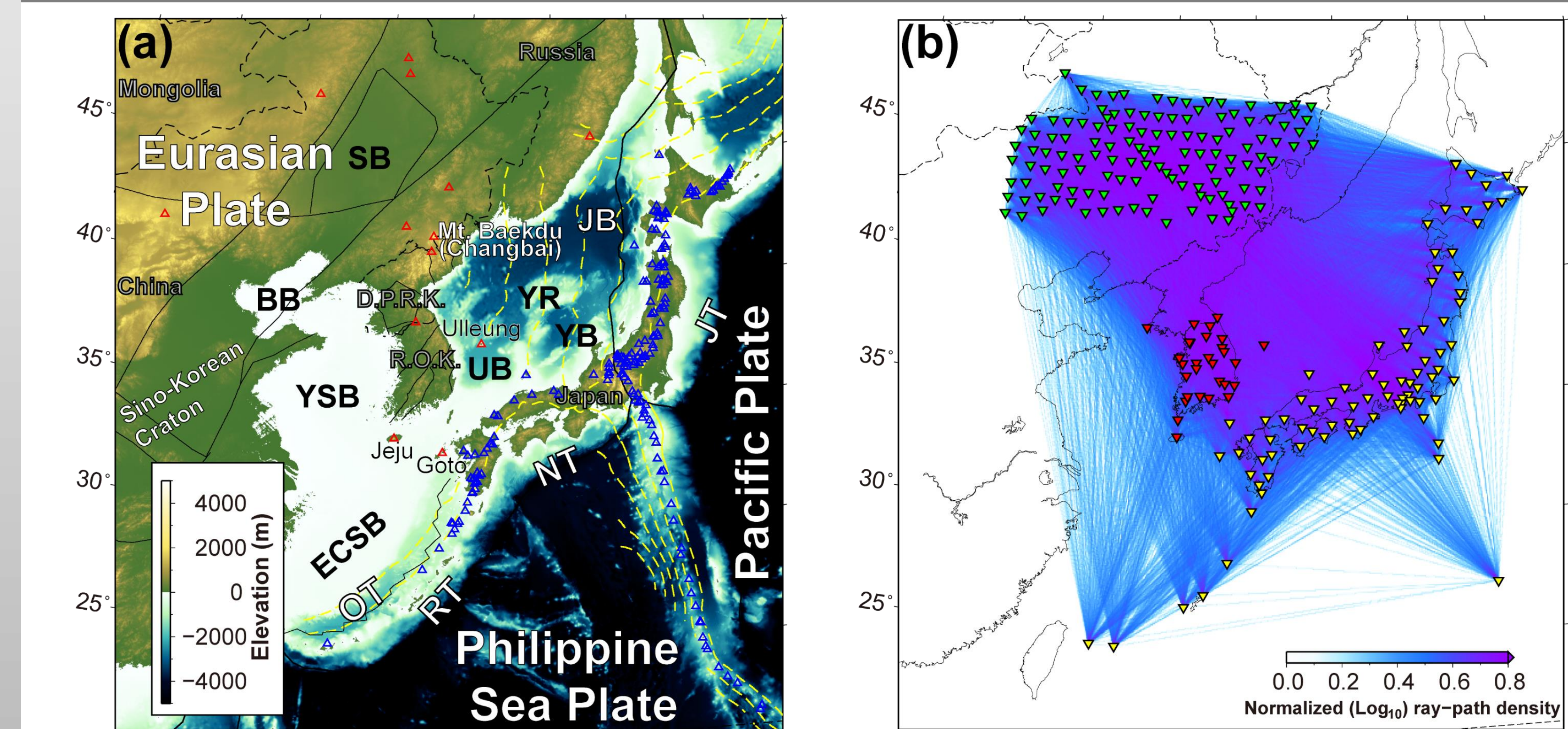


**Figure 1.** (a) Topographic map of the Northeast Asia region. The yellow contour indicates subduction depth of the Pacific plate and Philippine Sea plate. Features: SB, Songliao Basin; BB, Bohaiwan Basin; YSB, Yellow Sea Basin; ECSB, East China Sea Basin; UB, Ulleung Basin; JB, Japan Basin; YB, Yamato Basin; YR, Yamato Rise; RT, Ryukyu Trench; OT, Okinawa Trough; NT, Nankai Trough; JT, Japan Trench; Red triangles: intraplate volcanoes; Blue triangles: arc volcanoes. (b) All possible station pairs for cross-correlations. Receiver locations are shown by triangles for the following networks used in this study: F-net (yellow), KIGAM and KMA (red), and NECESSArray (green) stations.

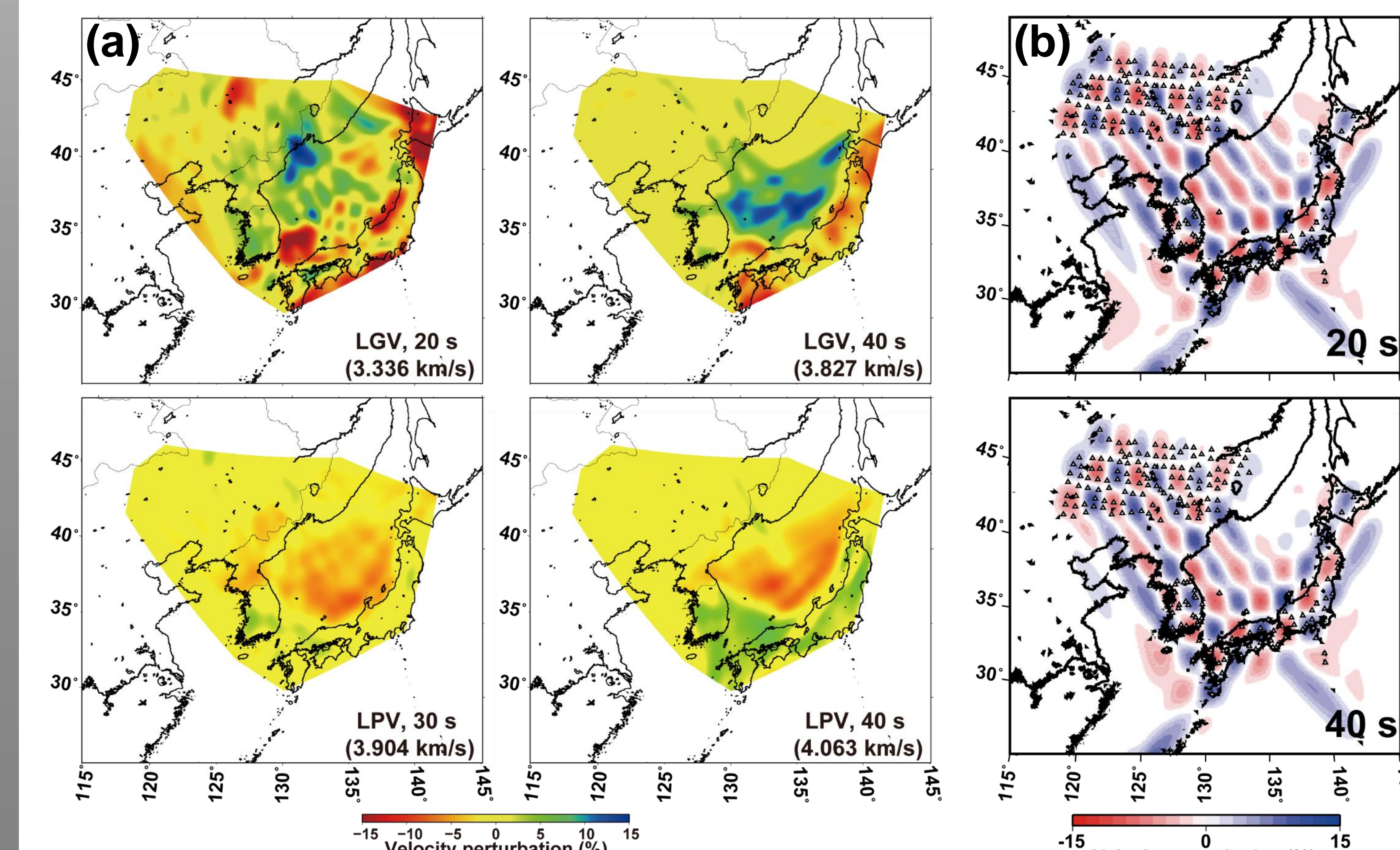


**Figure 2.** (a) Love wave group and phase velocity maps. (b) Checkerboard test results of synthetic tests for Love wave group and phase velocity at 20 and 40 s. Velocity maps were estimated using a nonlinear 2-D tomographic method, which combined a fast marching method and subspace inversion (Kennett et al., 1988; Rawlinson, 2005).

## 1D inversions and results

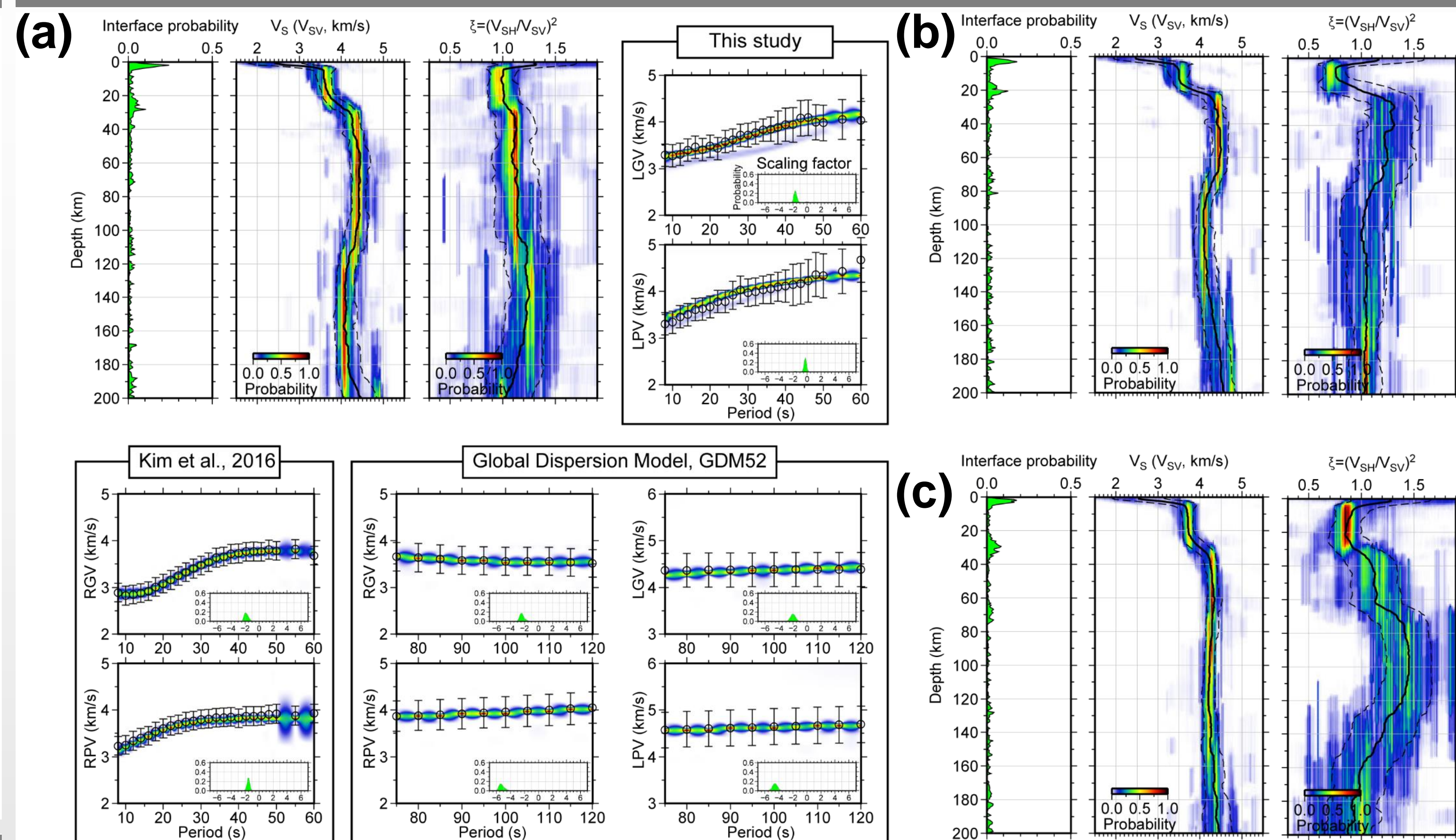


**Figure 3.** A series of one-dimensional (1-D) inversions were performed for 461 nodes over a geographical grid spacing 0.02°. The previously established Bayesian inversion technique of Kim et al. (2017) was used. In this method, fully nonlinear Markov chain Monte Carlo (MCMC) sampling is used without assuming arbitrary constraints (e.g., initial models). Also, different weightings are automatically imposed by searching for different noise levels in different types of data based on the information within the data. (a) The posterior probability distribution (PPD) of layer boundaries, shear wave velocity, anisotropy in depth and number of layer of the Bayesian inversion result using Rayleigh/Love wave dispersions at 34.9°N, 129.5°E. Rayleigh wave group velocity; RGW, Love wave group velocity; LGV, Rayleigh wave phase velocity; RPV, Love wave phase velocity; LPV (c) Posterior distributions of predicted synthetic data with observed data. Total 8 different types of dispersion maps of Love wave from this study (period 8-60 s), Rayleigh wave from previous tomographic study (Kim et al., 2016; period 8-60 s) and longer period data (period 70-120 s) from a global model (Ekstrom, 2011) are inverted together to estimate 1-D shear wave velocity models. (b) and (c) Results of 1-D shear velocity and anisotropy in depth for the Korean Peninsula, Ulleung Basin and Mt. Baekdu(Changbai) regions.

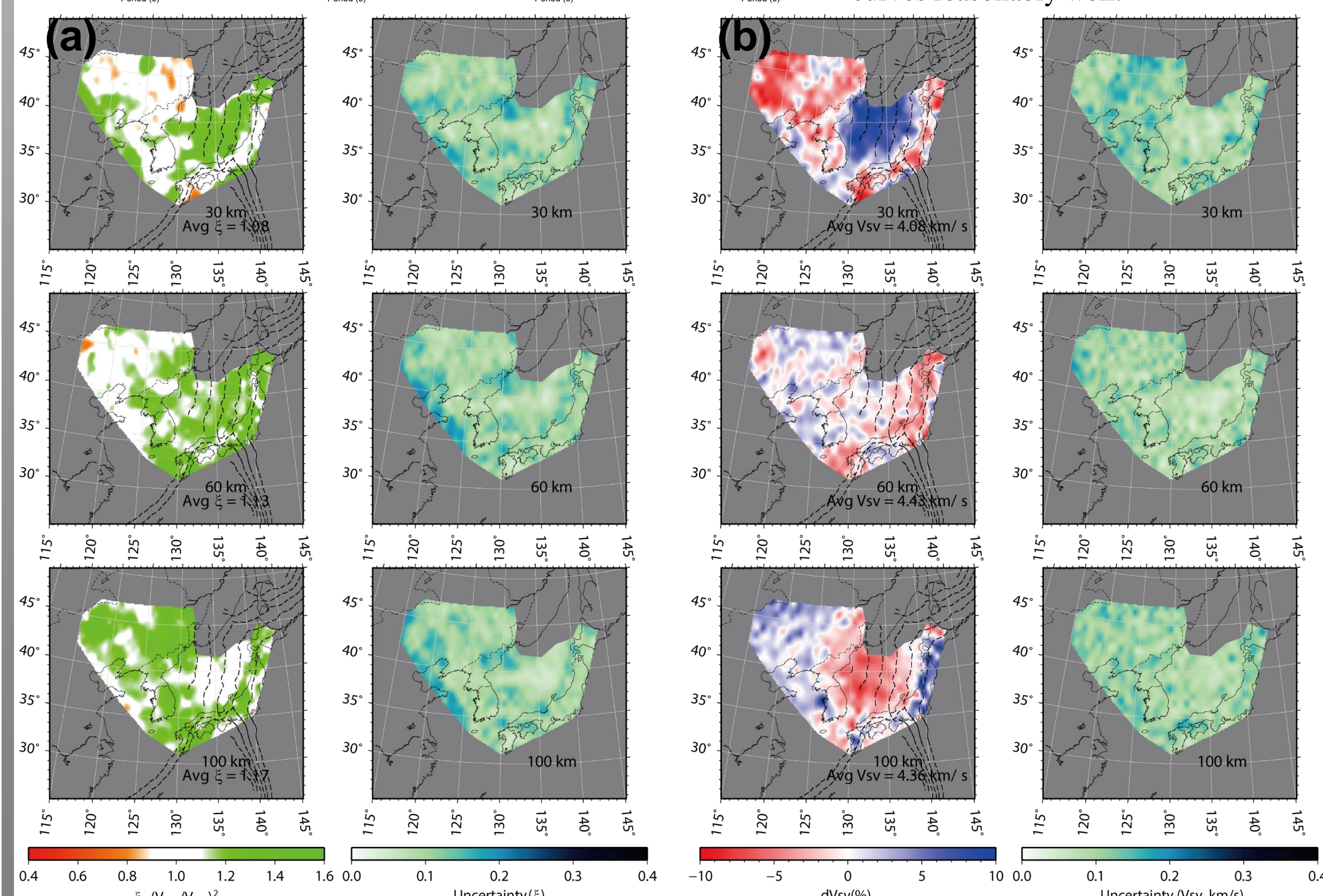
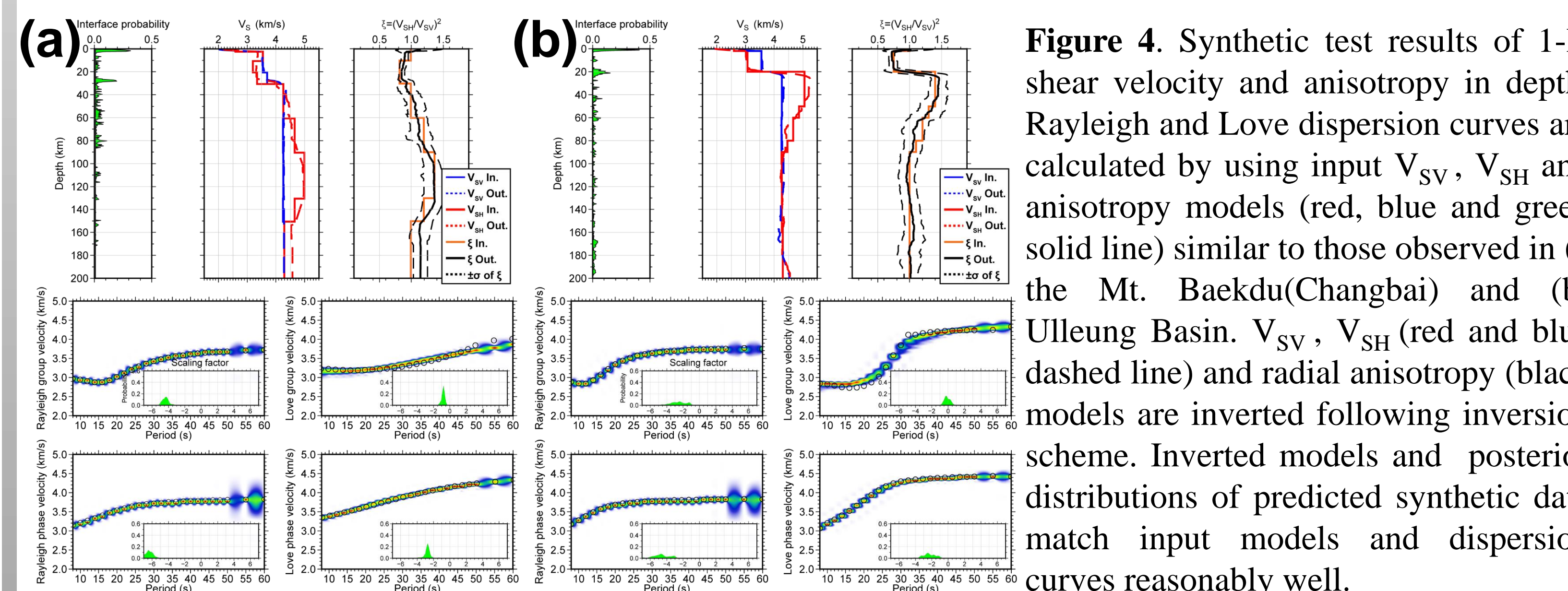


**Figure 5.** (a) Horizontal slices of the anisotropy model and uncertainties for NE Asia for selected depths. The depth and mean anisotropy are presented in right corner. (b) Horizontal slices of the Vsv model and uncertainties.

## Discussion

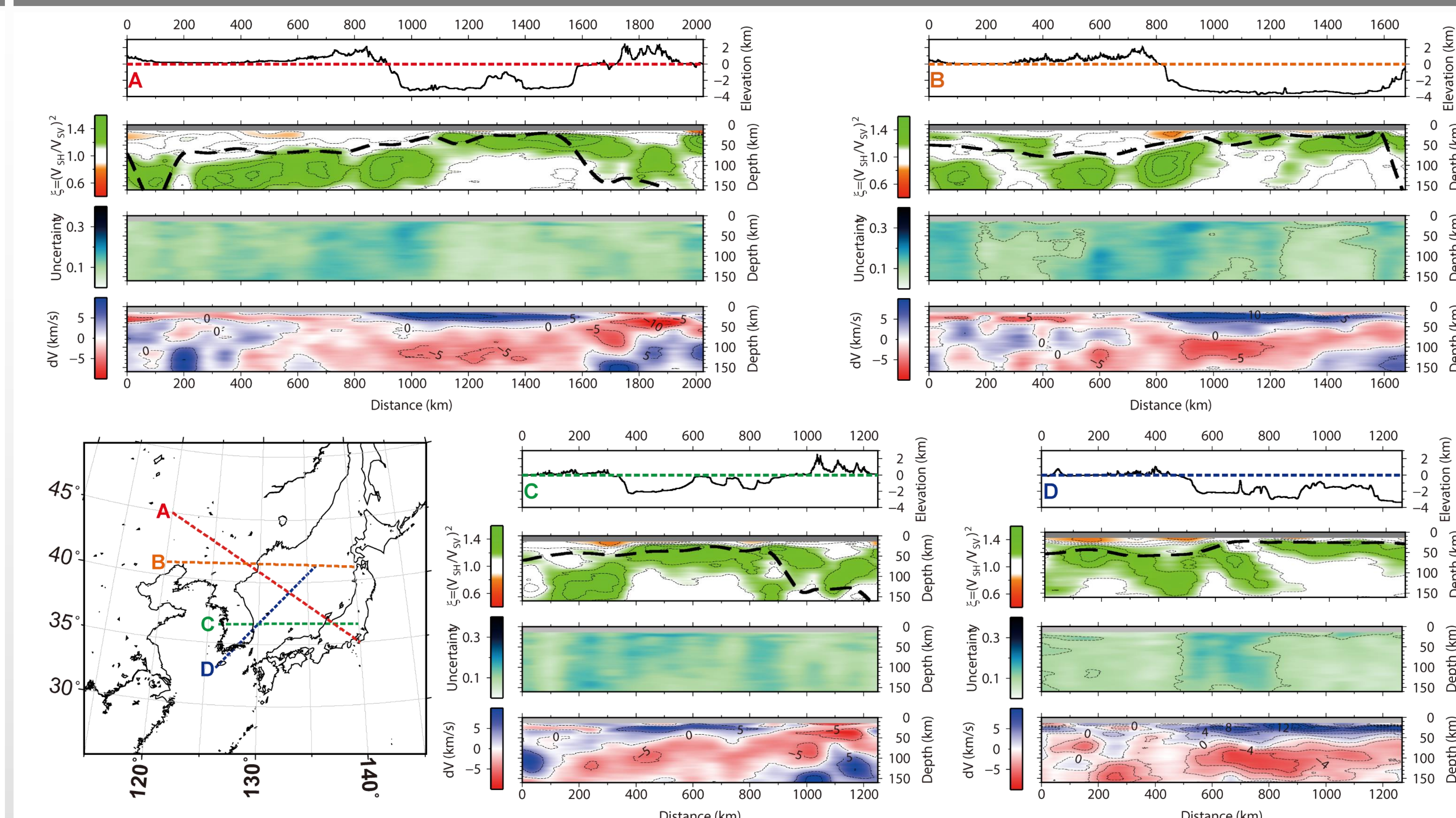


**Figure 6.** Vertical sections of the anisotropic models, uncertainties and relative Vsv models following profiles. LAB form Litho 1.0 is plotted with the anisotropic model (black dashed line).

### The difference of the thickness in the lithosphere around the East Sea (ES)

- The predominant depth of positive radial anisotropy was about 70–150 km in the inland area, while it was strong at shallower depth (20–70 km) and became weak as the depth deepened in the ES.
- The dominant positive radial anisotropy up to 70 km in the UB and YB seemed to represent a horizontally reset mantle fabric in the lithosphere with the horizontal flow in the upper part of the convection in the asthenosphere during the opening of the ES, while the horizontal flow beneath the lithosphere was disturbed by convection and was imaged as weak anisotropy

### Possible scenario for the Cenozoic volcanism in the NEA

- The Positive radial anisotropy beneath the intraplate volcanic regions can be divided into the one corresponded to the thickest corner of the continental lithosphere and the other located at the slope between western thick and eastern thin lithosphere (50-150 km).
  - EDC can occur if there is a difference of the thickness in lithosphere along the direction of horizontal flow in the asthenosphere and can caused intraplate volcanisms (King and Ritsema, 2000; Davies and Rawlinson, 2014).
- The subduction of the Pacific plate caused mantle wedge and the hot mantle upwelling intruded beneath the caused small-scale convection in the asthenosphere during the ES opening (from the Early Oligocene (~32 Ma) to about 15 Ma) and the lithosphere beneath the ES became thinned.
  - The difference of the thickness in lithosphere triggered the EDC and the magma supplied from the low velocity anomaly in the ES to the MBV and the other intraplate volcanoes (from ~20 Ma to present).
  - The magma supply through various depths could explain various compositional eruptions (from basalt to ignimbrite) from Miocene to Holocene.

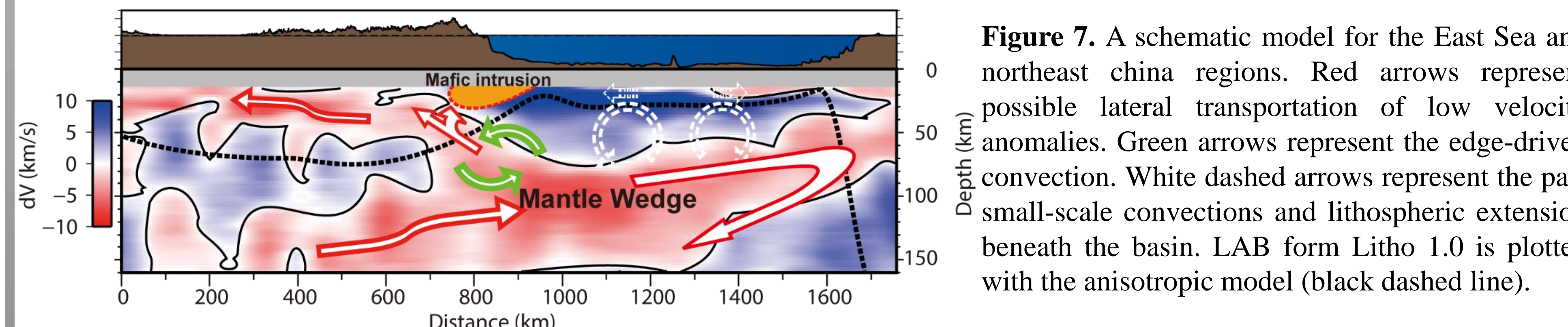


**Figure 7.** A schematic model for the East Sea and northeast China regions. Red arrows represent possible lateral transportation of low velocity anomalies. Green arrows represent the edge-driven convection. White dashed arrows represent the past small-scale convections and lithospheric extension beneath the basin. LAB form Litho 1.0 is plotted with the anisotropic model (black dashed line).

- In the case of Jeju Island (JI), a strong positive radial anisotropy, shallower (50–80 km) than the others, was located beneath JI and overlapped with the low-velocity anomaly.
- A thick lithosphere (>150 km) in the southwestern part of the KP also could be a possible cause basaltic intraplate volcanisms in JI associated with the effective viscosity changes of the asthenospheric flow near the thick lithosphere (Ballmer et al., 2015).

## References

Ballmer, M. D., Conrad, C. P., Smith, E. I., & Johnsen, R. (2015). Intraplate volcanism at the edges of the Colorado Plateau sustained by a combination of triggered edge-driven convection and shear-driven upwelling. *Geochemistry, Geophysics, Geosystems*, 16(2), 366-379.

Davies, D. R., & Rawlinson, N. (2014). On the origin of recent intraplate volcanism in Australia. *Geology*, 42(12), 1031-1034.

Ekström, G. (2011). A global model of Love and Rayleigh surface wave dispersion and anisotropy. *Geophysical Journal International*, 187(3), 1668-1686.

Kennett, B. L. N., Sambridge, M. S., & Williamson, P. R. (1988). Subspace methods for large inverse problems with multiple parameter classes. *Geophysical Journal International*, 94(2), 237-247.

Kim, S., Kralčić, H., Rhie, J., & Chen, Y. (2016). Intraplate volcanism controlled by back-arc and continental structures in NE Asia inferred from transdimensional Bayesian ambient noise tomography. *Geophysical Research Letters*, 43(16), 8390-8398.

Kim, S., Kralčić, H., & Rhie, J. (2017). Seismic constraints on magma evolution beneath Mount Baekdu (Changbai) volcano from transdimensional Bayesian inversion of ambient noise data. *Journal of Geophysical Research: Solid Earth*.

King, S. D., & Ritsema, J. (2000). African hot spot volcanism: small-scale convection in the upper mantle beneath cratons. *Science*, 290(5494), 1137-1140.

Rawlinson, N., & Sambridge, M. (2005). The fast marching method: an effective tool for tomographic imaging and tracking multiple phases in complex layered media.

## Acknowledgement

This work was funded by the Korea Meteorological Administration under grant KMIPA2017-4020